Applied Energy 217 (2018) 346–360

Contents lists available at ScienceDirect

Applied Energy

journal homepage: www.elsevier.com/locate/apenergy

Robust optimization for energy transactions in multi-microgrids under uncertainty

Bingying Zhang[a], Qiqiang Li[a,*], Luhao Wang[b], Wei Feng[c]

[a] School of Control Science and Engineering, Shandong University, Jinan 250061, China
[b] School of Electrical Engineering, University of Jinan, Jinan 250022, China
[c] Ernest Orlando Lawrence Berkeley National Laboratory, Berkeley, CA 94720-8136, USA

HIGHLIGHTS

- Formulated the multi-microgrid (MMG) operation as a transaction commitment problem.
- Designed a two-stage robust optimization based MMG coordinated operation approach.
- Described discrete feature of energy interactive behaviour among multiple microgrids.
- Mitigated the disturbances of uncertainties in renewable energy.
- Reduced frequent energy exchange between the MMG and the grid.

ARTICLE INFO

Keywords:
Multi-microgrid
Energy transaction
Uncertainty
Robust optimization
Unit commitment

ABSTRACT

Independent operation of single microgrids (MGs) faces problems such as low self-consumption of local renewable energy, high operation cost and frequent power exchange with the grid. Interconnecting multiple MGs as a multi-microgrid (MMG) is an effective way to improve operational and economic performance. However, ensuring the optimal collaborative operation of a MMG is a challenging problem, especially under disturbances of intermittent renewable energy. In this paper, the economic and collaborative operation of MMGs is formulated as a unit commitment problem to describe the discrete characteristics of energy transaction combinations among MGs. A two-stage adaptive robust optimization based collaborative operation approach for a residential MMG is constructed to derive the scheduling scheme which minimizes the MMG operating cost under the worst realization of uncertain PV output. Transformed by its KKT optimality conditions, the reformulated model is efficiently solved by a column-and-constraint generation (C&CG) method. Case studies verify the effectiveness of the proposed model and evaluate the benefits of energy transactions in MMGs. The results show that the developed MMG operation approach is able to minimize the daily MMG operating cost while mitigating the disturbances of uncertainty in renewable energy sources. Compared to the non-interactive model, the proposed model can not only reduce the MMG operating cost but also mitigate the frequent energy interaction between the MMG and the grid.

1. Introduction

Microgrids (MGs) integrated with distributed renewable energy generations and storage systems can effectively improve energy utilization and reduce environmental pollution [1–3]. Recently, as the technologies of roof-top PV and Electric Vehicle (EV) grow in popularity, the deployment of residential MGs is increasing [4,5]. Multiple neighbouring MGs appear in a local area and can be interconnected to form a multi-microgrid (MMG) for better energy performance [6–8]. Different from a single MG, for a MMG, energy can be exchanged not only with the grid but also among MGs, which makes the operation process of MMGs more complex. Moreover, most existing operating approaches for MMGs are based on deterministic conditions, which is hard to adapt to randomness of renewable energy sources (RESs). Overall, complicated mechanism and uncertainties in MMG operation may lead to various problems, such as low energy efficiency, high operation cost and frequent interaction with the grid. Therefore, in order to improve robustness and economy of MMG operation, it is necessary to design an effective operation method to coordinate the operation of multiple MGs and immunize against randomness of RESs.

* Corresponding author.
E-mail address: qqli@sdu.edu.cn (Q. Li).

https://doi.org/10.1016/j.apenergy.2018.02.121
Received 16 November 2017; Received in revised form 31 January 2018; Accepted 17 February 2018

Nomenclature

Indices

i,j	index of MGs
t	index of hours

Sets

G	set of MGs, $i,j \in G, G = \{1,2,...,n\}$
T	set of time intervals, $t \in T, T = \{0,1,...,23\}$
T_P	intervals when the EV is plugged, $T_P \subseteq T, T = \{t_1, t_1+1, ..., t_2-1\}$

Binary variables

$r(i,j,t)$	binary variable of MG i related to the power exchange status between MG i and MG j, $r(i,j,t) = 1$ if MG i purchases power from MG j at time t, $r(i,j,t) = 0$ otherwise
$s(i,j,t)$	binary variable of MG i related to the power exchange status between MG i and MG j, $s(i,j,t) = 1$ if MG i sells power to MG j at time t, $s(i,j,t) = 0$ otherwise
$u(i,t)$	binary variable of MG i related to the power exchange status between MG i and the grid, $u(i,t) = 1$ if MG i purchases power from the grid at time t, $u(i,t) = 0$ otherwise
$v(i,t)$	binary variable of MG i related to the power exchange status between MG i and the grid, $v(i,t) = 1$ if MG i sells power to the grid at time t, $v(i,t) = 0$ otherwise
$z(i,t)$	binary variable related to charging status of EV in MG i, $z(i,t) = 1$ if EV in MG i is charging at time t, $z(i,t) = 0$ otherwise
$w(i,t)$	binary variable related to discharging status of EV in MG i, $w(i,t) = 1$ if EV in MG i is discharging at time t, $w(i,t) = 0$ otherwise

Continuous variables

TC	expected daily total cost of multiple MGs (CNY)
$p_{mb}(i,j,t)$	power that MG i purchases from MG j at time t (kW)
$p_{ms}(i,j,t)$	power that MG i sells to MG j at time t (kW)
$p_{gb}(i,t)$	power that MG i purchases from the grid at time t (kW)
$p_{gs}(i,t)$	power that MG i sells to the grid at time t (kW)
$p_{ec}(i,t)$	charging power of EV in MG i at time t (kW)
$p_{ed}(i,t)$	discharging power of EV in MG i at time t (kW)
$SOC_{ev}(i,t)$	state of charge of EV in MG i at time t (%)
$p_{pv}(i,t)$	actual power output of PV in MG i at time t (kW)

Parameters

Δ_T	duration of time intervals. In this paper, $\Delta_T = 1$ h.
$P^f_{pv}(i,t)$	predicted power output of PV in MG i at time t (kW)
$\Delta_{pv}(i,t)$	deviation from the predicted PV power output in MG i at time t (kW)
$\Gamma(i)$	budget of uncertainty of PV in MG i
$P_l(i,t)$	predicted load demand in MG i at time t (kW)
$C_{pv}(i)$	O&M cost of PV in MG i (CNY/kW h)
$C_{ev}(i)$	charging/discharging cost of EV in MG i (CNY/kW h)
a_{ser}	service charge of exchange between MGs (CNY)
b_{ser}	service charge of exchange between MG i and the grid (CNY)
$c_m(t)$	electricity price among MGs at time t (CNY/kW h)
$c_{gb}(t)$	purchasing electricity price from the grid at time t (CNY/kW h)
$c_{gs}(t)$	selling electricity price to the grid at time t (CNY/kW h)
$cost_0(i)$	electricity cost of MG i in the MMG without energy exchanging (CNY)
P^{max}_m	exchanging power limit between MGs (kW)
P^{max}_{gb}	purchasing power limit from the grid (kW)
P^{max}_{gs}	selling power limit to the grid (kW)
t_1	the time at which EVs are plugged in
t_2	the time at which EVs depart
$P^{max}_{ec}(i)$	maximum charging power of EV in MG i (kW)
$P^{max}_{ed}(i)$	maximum discharging power of EV in MG i (kW)
$\eta_{ec}(i)$	charging efficiency of EV in MG i (%)
$\eta_{ed}(i)$	discharging efficiency of EV in MG i (%)
$Cap_{ev}(i)$	capacity of battery of EV in MG i (kW h)
$SOC^{max}_{ev}(i)$	maximum state of charge of EV in MG i (%)
$SOC^{min}_{ev}(i)$	minimum state of charge of EV in MG i (%)
$SOC_{ev}(i,t_1)$	initial state of charge of EV in MG i at time t_1 (%)
$SOC_{ev}(i,t_2)$	users' desired SOC of EV in MG i at time t_2 (%)

1.1. Literature review

Recently, there have been increasing researches focusing on MMG operation approaches. According to energy interaction relationships among MGs, these researches can be classified into non-interactive [9–15] and interactive [16–19]. For non-interactive MMGs, MGs directly exchange energy with the grid without considering local energy interaction. To avoid electricity exchange peaks, decentralized energy scheduling strategies between a multi-microgrid system and the grid are studied in [9,10]. To simultaneously maximize the interests of the MMG, the distribution network operator (DNO) and the grid, [11] develops a multi-objective approach, [12,13] propose bi-level optimization methods, and [14] designs a distributed economic model predictive control scheme. Besides economic objectives, [15] also considers security guarantee in its proposed new modeling framework by dynamically estimating the power interchange between MMGs and a DNO. From the perspective of future smart grids, the joint operation with energy interaction among MGs is preferable to the independent operation of single MGs, which ensures greater operation benefits and energy efficiency. A memetic algorithm based approach for a building-level microgrid cluster is presented in [16] to achieve local sharing of cooling energy. Similarly, an augmented multi-objective particle swarm optimization framework for the same system is developed in [17] to achieve thermal energy sharing among MGs. In [18,19], connection between MGs is considered in MMG optimal scheduling to enable their power sharing in an interconnected operation mode. These researches demonstrate that interactive operation methods can improve economy and operation performance, therefore, how to more effectively guide and motivate energy transactions among MGs becomes hot research topics.

To optimize energy transactions among multiple MGs, several energy trading modes have been designed, which can be generally classified into competitive modes [20,21] and cooperative modes [22–26]. By passing the profit margin of each MG to energy service provider, the competitive situation of multiple MGs is formulated as a bi-level programming [20]. Considering different consumer preferences and loads in buildings, the non-cooperative game theory is introduced in the joint operation of multiple buildings with PV systems [21]. However, for most competitive modes, the overall efficiency of MMGs is not considered, which may lead to energy waste. Therefore, cooperative modes among multiple MGs are investigated based on flexible price mechanisms. Such as, [22] defines Lagrange multipliers as dynamic purchase prices for power transactions among MGs. [23] proposes a distributed energy trading method for a MMG based on dual decomposition, in which energy prices are adjusted according to the law of demand. Along this line, a parallel optimization strategy for multiple buildings is developed by introducing Lagrange multipliers for energy exchange in all transmission lines [24]. In [25], an interactive energy game matrix is

proposed to describe operational interaction of networked MGs. In addition to absorb the redundant energy within MMGs, the cooperative mode can also allocate the desired power to support the on-emergency MG in a MMG [26]. Usually, energy interaction might not occur simultaneously in all MGs since different MGs have distinctive operation benefits, so the combination of energy transactions among MGs needs to be considered in MMG operation. However, most existing works do not take into account the characteristics of energy transactions among MGs, and lack a systematic commitment and operation optimization process of MMGs. In this paper, the characteristics of discrete combinations of energy transactions among multiple MGs is considered from the system point of view. Thus, the MMG operation problem is formulated as a unit commitment (UC) optimization problem, in which each MG is treated as a generation unit with bi-directional power flow.

Besides, in MMG operation, uncertainties can bring about not only challenges to maintain the supply-demand balance but also adverse impacts on energy transaction decisions. To manage uncertainties in MMG operation, several techniques are introduced to design operation approaches. For example, [27] presents a data-driven feed-forward decision framework for a building cluster to study energy sharing under uncertainty. However, requiring large amounts of training data and long training time makes it not applicable to short-time scale operation scheduling of MGs. In [28], a stochastic decision model is formulated for economic operation of a multi-microgrid system, where uncertainties in load and RESs are modeled by probability density functions (PDFs). In [29], the stochastic nature of RESs, loads, and prices is also modeled based on their PDFs to optimize the operation of distribution networks under MMGs concept. [24] tackles uncertainties in the jointly operation of multiple buildings by a scenario-based method. However, stochastic operation methods require a huge number of scenarios to obtain accurate probability distributions of uncertainties, which may lead to computational complexity and produce high computational cost. To avoid these limitations, robust optimization (RO) is applied to address uncertainty in MGs and power systems effectively. Capturing uncertainty with predefined uncertainty sets instead of probability distributions, RO doesn't need numerous samples of historical measured data [30]. In [31], a RO based MG energy management is implemented, which significantly improves system operation performance by considering the worst realization of uncertainty. A robust optimization approach is also adopted in [32] to accommodate wind power uncertainty and achieve cost minimization in MGs. [33] presents a robust multi-objective optimization approach for a MG supply and demand scheduling problem under uncertainty. Furthermore, multiple uncertainty sets are used in [34] to simplify the acquisition of uncertain data in practical applications and adaptive robust sets are designed in [35] to control conservatism of the robust solution. And [36] constructs computationally friendly uncertainty sets from sample data by data-driven RO approach. In this paper, we also employ an adaptive robust optimization (ARO) approach to capture PV uncertainty by an uncertainty set with parameter *budget of uncertainty*.

1.2. Contributions and organization

This paper proposes a robust optimization based approach for optimal MMG operation in a residential scenario considering renewable energy uncertainty and interactive behaviours of energy among MGs. An adapted UC model is utilized to describe the complicated transaction relationships among multiple interconnected MGs. Thus, MGs can be scheduled to operate collaboratively and exchange energy reasonably to minimize the MMG operation cost. To the best of our knowledge, there has been no comprehensive research to incorporate both the discrete and continuous features in MMG operation while dealing with uncertainty. The main contributions of this paper can be summarized as follows:

- The MMG transaction coordination and economic operation problem is formulated as a UC problem, which achieves coordinative operation of multiple MGs to reduce operating cost and energy exchange with the grid.
- A two-stage adaptive robust optimization formulation for a MMG is presented to make upper-level discrete commitment decisions and lower-level continuous operation decisions as well as mitigate the disturbance of intermittent renewable energy.
- Based on KKT optimality conditions, the MMG optimization model is transformed to mixed integer linear programming (MILP), which can be successfully solved by existing cutting-plane decomposition algorithms to find exact solutions.

The remainder of this paper is organized as follows. Section 2 describes the problem briefly about the MMG architecture and relevant assumptions. A mathematical formulation is developed in Section 3. In Section 4, we present the transformation of the model and its solving algorithm. Case studies and numerical results are shown in Section 5. Finally, Section 6 concludes our research.

2. Problem statement

In this paper, the MMG under study consists of multiple interconnected home MGs in a residential area, in which there exist interactive behaviours of energy among MGs. As shown in Fig. 1, each MG contains a roof-top PV, a plug-in electric vehicle (PEV) and domestic loads. The PEV is plugged in only once and for a consecutive period every single day, during which it behaves as a storage unit. Moreover, inverters and a local controller is integrated in the 'I-box' of each house.

In each MG, the load is first fulfilled by its own PV, then if there is excessive electricity from PV, it can be used to charge the PEV battery or sell to other MGs or the grid through the aggregator, and vice versa. Due to the randomness of PV generation, its output power is considered as uncertainty in the MG operation. The local energy transactions among MGs are managed by an aggregator, which also acts as an agent for the MMG to exchange energy with the grid. In general, the aggregator's optimizer is high-performance computer integrated the scheduling approach. The aggregator transmits the information such as electricity prices, demands and control signals between houses and the grid through a communication network. Due to the information and energy management, line capacity and other relevant services provided by the aggregator, a fixed service charge is occurred for the two sides of the energy transaction. The flow of payment, energy and information in the MMG is illustrated in Fig. 2.

The problem formulation takes into account not only interactive

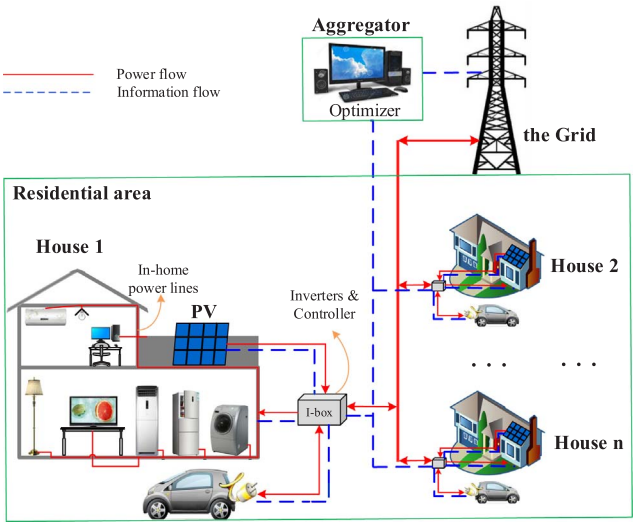

Fig. 1. The structure of a residential MMG.

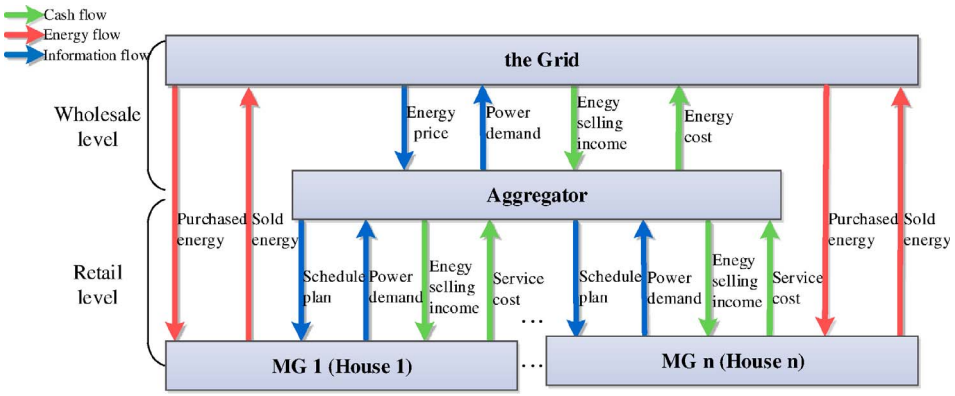

Fig. 2. The flow of cash, energy and information in the MMG.

behaviours of energy between the MGs and the grid, but also energy transactions among MGs. The goal of our study is to derive the optimal collaborative operating scheme in order to minimize the total operation cost of the MMG while mitigating disturbance of PV uncertainty. Therefore, the main decisions to be made for each MG include:

(1) Whether to exchange power with other MGs and the amount of power to be purchased/sold in each time interval *t*.
(2) Whether to exchange power with the grid and the amount of power to be purchased/sold in each time interval *t*.
(3) Whether to charge/discharge the PEV and the amount of power to be charged/discharged in each time interval *t*.

From the system point of view, we can treat each MG as an individual generation unit that has bi-directional power interaction with the grid or other MGs. Then, the MMG can be seen as a power system containing multiple generation units. Therefore, this problem is similar to the unit commitment problem in the power system area, which involves determining the ON/OFF status (discrete commitment decisions) first and then the generation level (continuous production decisions) for each generator over a given period of time. Given this consideration, the status of energy exchange can be seen as the ON/OFF status of generation units, the amount of exchanged electricity can be seen as the output power of generation units in the UC problem. Then, considering PV uncertainty, a two-stage adaptive robust optimization model is formulated.

Compared with the conventional UC problem in power systems, the adapted UC problem in MMGs is more complicated. Firstly, different from a conventional generator, each MG has to meet its internal power balance constraint, which increases the burden of solving this problem. Secondly, a MG's UC decisions would be influenced by the operation of other MGs and the grid, because it has to decide whether to trade energy with them. Thirdly, after energy transactions within MMGs, the power balance may not be satisfied and need further transactions with the grid, which leads to a complicated two-level scheduling problem. So, it can be called transaction commitment problem in this work. Besides, the two-stage robust formulation hedges against the uncertainty of PV generation by including a large number of scenarios in the uncertainty set, which also leads to a hard-to-solve large-scale problem.

Both the detailed mathematical model and its compact matrix format will be described in the next section.

3. Mathematical formulation

In this section, we develop a two-stage adaptive robust optimization model to study the energy exchanging and collaborative operation among multiple MGs under the uncertain PV outputs. We first give all the constraints of the optimization model and the definition of PV uncertainty set. Then the complete two-stage adaptive robust formulation of the MMG collaborative operation problem will be presented. The variables and parameters defined in the proposed model are listed and explained in Nomenclature and all of them are nonnegative.

3.1. Constraints

3.1.1. Exchange constraints

As described above, a single MG can be seen as a schedulable generator which has bidirectional power flow and be scheduled in its entirety. To avoid using negative-value variables, four continuous variables are defined to represent the exchanged power of a single MG, which are the power purchased from other MGs, the power sold to other MGs, the power purchased from the grid and the power sold to the grid, respectively. Also, the corresponding binary variables are defined to represent power exchange statuses of a single MG.

(1) Exchange status constraints

For a single MG, purchasing and selling power cannot be simultaneously. Thus, the exchange status of every MG should satisfy the following inequations.

$$r(i,j,t) + s(i,j,t) \leqslant 1\,, \quad \forall\, i,j \in G, \quad j \neq i\,, \forall\, t \in T \tag{1}$$

$$u(i,t) + v(i,t) \leqslant 1\,, \quad \forall\, i \in G\,, \quad \forall\, t \in T \tag{2}$$

where if $r(i,j,t) = s(i,j,t) = 0$, there is no power exchange between MG i and MG j. Else, if either of $r(i,j,t)$ and $s(i,j,t)$ equals to 1, there exists power exchange between them. Likewise, if $u(i,t) = v(i,t) = 0$, there is no power exchange between MG i and the grid. Else, if either of $u(i,t)$ and $v(i,t)$ equals to 1, there exists power exchange between them.

Remark. A MG can purchase power from other MGs and/or from the grid in the same time interval, and it can sell power to other MGs and/or to the grid simultaneously as well.

(2) Exchange power capacity constraints

Due to line capacities, technical limits of inverter interfaces and contracted limits of power exchange, MGs have output limits which the exchanged power cannot exceed.

$$0 \leqslant p_{mb}(i,j,t) \leqslant r(i,j,t) P_m^{max}\,, \quad \forall\, i,j \in G, \quad j \neq i\,, \quad \forall\, t \in T \tag{3}$$

$$0 \leqslant p_{ms}(i,j,t) \leqslant s(i,j,t) P_m^{max}\,, \quad \forall\, i,j \in G, \quad j \neq i\,, \quad \forall\, t \in T \tag{4}$$

$$0 \leqslant p_{gb}(i,t) \leqslant u(i,t) P_{gb}^{max}\,, \quad \forall\, i \in G\,, \quad \forall\, t \in T \tag{5}$$

$$0 \leqslant p_{gs}(i,t) \leqslant v(i,t) P_{gs}^{max}\,, \quad \forall\, i \in G\,, \quad \forall\, t \in T \tag{6}$$

In addition, the power purchased by MG i from MG j is the same power sold by MG j to MG i.

$$p_{mb}(i,j,t) = p_{ms}(j,i,t)\,, \quad \forall\, i,j \in G, \quad j \neq i\,, \quad \forall\, t \in T \tag{7}$$

(3) Individual interests of each MG

To ensure that each MG joining power exchange won't spend more money than in independent operation, we add the following constraint.

$$\sum_{t=0}^{23}\sum_{j=1,j\neq i}^{n}(r(i,j,t)+s(i,j,t))a_{ser}+\sum_{t=0}^{23}(u(i,t)+v(i,t))b_{ser}+\sum_{t=0}^{23}p_{pv}(i,t)C_{pv}(i)+\sum_{t=0}^{23}(p_{ec}(i,t)+p_{ed}(i,t))C_{ev}(i)+\sum_{t=0}^{23}\sum_{j=1,j\neq i}^{n}(p_{mb}(i,j,t)-p_{ms}(i,j,t))c_m(t)+\sum_{t=0}^{23}(p_{gb}(i,t)c_{gb}(t)-p_{gs}(i,t)c_{gs}(t))\leqslant cost_0(i),\quad \forall i\in G,\quad \forall t\in T \tag{8}$$

where $cost_0(i)$ is the cost of the MG i in the MMG where multiple MGs are disconnected and thus there is no power exchanging among MGs. Its value can be solved from the independent operation model of MMGs, in which power interactions among MGs is not allowed (called Non-interactive Model or NI-Model and listed in Appendix A).

3.1.2. Power balance constraints

(1) Power balance of the MMG

For the MMG, the total power production and consumption should satisfy the following power balance equation.

$$\sum_{i=1}^{n}P_l(i,t)+\sum_{i=1}^{n}p_{ec}(i,t)+\sum_{i=1}^{n}p_{gs}(i,t)=\sum_{i=1}^{n}p_{pv}(i,t)+\sum_{i=1}^{n}p_{ed}(i,t)+\sum_{i=1}^{n}p_{gb}(i,t),\quad \forall i\in G,\quad \forall t\in T \tag{9}$$

The left-hand side of (9) collects the total consumption of the MMG at time t: the total load of all the MGs, the total power charged to all the EVs and the total power sold to the grid. The right-hand side consists of the total available power in the MMG at time t: the total PV generation from all the MGs, the total discharged power from the EVs and the total power purchased from the grid.

(2) Power balance of MG i

For each MG in the MMG, the supply should also meet its demand.

$$P_l(i,t)+p_{ec}(i,t)+\sum_{j=1,j\neq i}^{n}p_{ms}(i,j,t)+p_{gs}(i,t)=p_{pv}(i,t)+p_{ed}(i,t)+\sum_{j=1,j\neq i}^{n}p_{mb}(i,j,t)+p_{gb}(i,t),\quad \forall i,j\in G,\quad \forall t\in T \tag{10}$$

The left-hand side of (10) represents the total consumption of MG i at time t which consists of the load in MG i, the power charged to the EV in MG i, the total power sold to other MGs and the power sold to the grid. The right-hand side consists of the total available power in MG i at time t: the PV generation of MG i, the power discharged from its EV, the total power purchased from other MGs and the power purchased from the grid.

3.1.3. EV constraints

As mentioned in Section 2, each EV is assumed to be plugged only once and for a consecutive period every single day, which means that the EV in every MG is plugged at time t_1, and departs at time t_2. To motivate PEV owners to participate in this discharging program, the aggregator would provide incentives to ensure that they make more money when joining the service than they do not. Here, we do not include the incentive price in our model since its calculating method exceeds our scope.

(1) EV battery capacity limit

$$SOC_{ev}^{min}(i)\leqslant SOC_{ev}(i,t)\leqslant SOC_{ev}^{max}(i),\quad \forall i\in G,\quad \forall t\in T \tag{11}$$

(2) EV battery charging/discharging status constraint

In each scheduling interval, the EV's charging and discharging are not simultaneous, which means that it is either charging or discharging. Note that in unplugged period, neither charging nor discharging is happening. Thus, the charging and discharging status must meet the following constraints.

$$z(i,t)+w(i,t)\leqslant 1,\quad \forall i\in G,\quad \forall t\in T \tag{12}$$

$$z(i,t)=w(i,t)=0,\quad \forall i\in G,\quad \forall t\in T\backslash T_P \tag{13}$$

(3) EV battery charging/discharging rate limits

The charging and discharging power limits are given as follows.

$$0\leqslant p_{ec}(i,t)\leqslant z(i,t)P_{ec}^{max}(i),\quad \forall i\in G,\quad \forall t\in T \tag{14}$$

$$0\leqslant p_{ed}(i,t)\leqslant w(i,t)P_{ed}^{max}(i),\quad \forall i\in G,\quad \forall t\in T \tag{15}$$

As shown in (14) and (15), if the charging or discharging status variable is zero, the corresponding charging or discharging power equals to zero likewise.

(4) Battery energy balance

In the plugged period, the update of the EV batteries' SOC must satisfy the battery energy balance constraint (16). The energy conversion efficiencies in the charging and discharging process are also considered.

$$SOC_{ev}(i,t+1)Cap_{ev}(i)=SOC_{ev}(i,t)Cap_{ev}(i)+\eta_{ec}(i)p_{ec}(i,t)\Delta_T-\frac{1}{\eta_{ed}(i)}p_{ed}(i,t)\Delta_T,\quad \forall i\in G,\quad \forall t\in T_P \tag{16}$$

(5) Initial and final SOC equality constraint during plugged period

Each EV battery has an initial value of SOC when it is plugged in the MG. Also, to satisfy the travel demand of EV users, a desired departure value of SOC should be set. Thus, the battery should satisfy the following equation throughout the whole plugged period.

$$SOC_{ev}(i,t_1)Cap_{ev}(i)+\sum_{t=t_1}^{t_2-1}\left(\eta_{ec}(i)p_{ec}(i,t)\Delta_T-\frac{1}{\eta_{ed}(i)}p_{ed}(i,t)\Delta_T\right)=SOC_{ev}(i,t_2)Cap_{ev}(i),\quad \forall i\in G,\quad \forall t\in T_P \tag{17}$$

where $SOC_{ev}(i,t_1)$ is the initial SOC of EV in MG i when it is plugged in at time t_1, and it can be measured by the smart meter at the EV plug. $SOC_{ev}(i,t_2)$ is the desired SOC set by users of MG i, which means the SOC must reach this value when the EV departs at time t_2.

3.2. Uncertainty set of PV output

Here, we introduce a robust set to describe the random power output of PVs. A very popular way to build an uncertainty set is to employ a predefined integer-value parameter called *budget of uncertainty* to impose the constraint and control the degree of conservatism [30,37].

$$\mathbf{U}=\left\{\boldsymbol{p_{pv}}\in R^{|G|\times|T|}:\sum_{t}\frac{|p_{pv}(i,t)-P_{pv}^{f}(i,t)|}{\Delta_{pv}(i,t)}\leqslant\Gamma(i),\forall i\in G\quad P_{pv}^{f}(i,t)-\Delta_{pv}(i,t)\leqslant p_{pv}(i,t)\leqslant P_{pv}^{f}(i,t)+\Delta_{pv}(i,t),\forall i\in G,\forall t\in T\right\} \tag{18}$$

$P_{pv}^{f}(i,t)$ is the forecasted PV output in MG i at time t,$\Delta_{pv}(i,t)$ is the deviation from the forecasted values of PV output, and the actual PV output $p_{pv}(i,t)$ can vary freely in interval $[P_{pv}^{f}(i,t)-\Delta_{pv}(i,t),P_{pv}^{f}(i,t)+\Delta_{pv}(i,t)]$. $\Gamma(i)$ is the *budget of uncertainty* for the PV in MG i, which is defined to take an integer value. Its value restricts the number of time intervals in which the PV output can deviate from its forecasted value. For instance, if $\Gamma(i)=0$, then the PV output of MG i can be considered equal to the forecasted value

throughout the whole sunlight period. If $\Gamma(i) = 5$, then the PV output of MG i are assumed to fluctuate in no more than 5 time intervals of the whole sunlight period. Therefore, the conservative level of the model can be controlled by adjusting the value of $\Gamma(i)$.

3.3. Optimization model

Based on the above-mentioned constraints and uncertainty set, the complete model is described as follows. This two-stage adaptive robust optimization model means that the *buy/sell* decisions are made first, and then, based on the first-stage decisions, the optimal amount of purchased/sold power can be determined to minimize the total MMG operating cost under various realizations of the uncertain factor that maximizes the cost.

$$\begin{aligned} TC = \min_{\boldsymbol{r},\boldsymbol{s},\boldsymbol{u},\boldsymbol{v},\boldsymbol{z},\boldsymbol{w}} & \sum_{t=0}^{23}\sum_{i=1}^{n}\left(\sum_{j=1,j\neq i}^{n}(r(i,j,t)a_{ser} + s(i,j,t)a_{ser}) + u(i,t)b_{ser}\right. \\ & \left. + v(i,t)b_{ser}\right) + \max_{\mathbf{U}}\min_{\boldsymbol{\Omega}}\sum_{t=0}^{23}\sum_{i=1}^{n}(p_{pv}(i,t)C_{pv}(i) \\ & + (p_{ec}(i,t) + p_{ed}(i,t))C_{ev}(i) + p_{gb}(i,t)c_{gb}(t) - p_{gs}(i,t)c_{gs}(t)) \end{aligned} \tag{19}$$

s.t.

(1)(2)(12)(13)

where

$$\boldsymbol{\Omega}(\boldsymbol{r},\boldsymbol{s},\boldsymbol{u},\boldsymbol{v},\boldsymbol{z},\boldsymbol{w},\boldsymbol{p}_{pv}) = \{(\boldsymbol{p}_{ec},\boldsymbol{p}_{ed},\boldsymbol{p}_{mb},\boldsymbol{p}_{ms},\boldsymbol{p}_{gb},\boldsymbol{p}_{gs},\boldsymbol{SOC}_{ev}):(3)\text{-}(11),(14)\text{-}(17)\}$$

in which, the bold font variables in set $\boldsymbol{\Omega}$ represent the vector forms of the corresponding variables, e.g., $\boldsymbol{r}$ represents variable $r(i,j,t)$, $\boldsymbol{p}_{ec}$ represents variable $p_{ec}(i,t)$.

The objective function formulated in (19) represents the daily MMG operating cost, which equals to the sum of the energy cost of every single MG in the MMG. For a single MG, its energy cost involves the following four terms: the cost of energy transaction among MGs, the cost of energy transaction with the grid, the operation and maintenance (O&M) cost of PVs, the charging and discharging cost of EVs' batteries. Note that the cost of energy transaction includes both the fixed service charge of the aggregator and the energy cost, as mentioned in Section 2.

Remark. For the MMG, the total cost of energy transaction among MGs is equal to the sum of fixed service charges, which is because the purchasing and selling electricity price in the local energy transaction is the same and the total amount of energy purchased from MGs equals to the total amount of energy sold to MGs.

3.4. Compact formulation

For simple exposition in the subsequent section, we give a compact matrix formulation of the above model as follows.

$$\min_{\boldsymbol{x}} \quad \boldsymbol{a}^{\mathrm{T}}\boldsymbol{x} + \max_{\boldsymbol{d}\in\mathbf{D}}\min_{\boldsymbol{y}\in\boldsymbol{\Omega}(\boldsymbol{x},\boldsymbol{d})}\boldsymbol{b}^{\mathrm{T}}\boldsymbol{y} \tag{20}$$

$$\text{s.t.} \quad \boldsymbol{C}\boldsymbol{x} \leqslant \boldsymbol{g}, \quad \boldsymbol{x} \in \{0,1\} \tag{21}$$

where

$$\boldsymbol{\Omega}(\boldsymbol{x},\boldsymbol{d}) = \{\boldsymbol{y}: \boldsymbol{E}\boldsymbol{y} \leqslant \boldsymbol{e} \tag{22}$$

$$\boldsymbol{A}\boldsymbol{y} + \boldsymbol{B}\boldsymbol{d} = \boldsymbol{c} \tag{23}$$

$$\boldsymbol{E}\boldsymbol{x} + \boldsymbol{F}\boldsymbol{y} \leqslant \boldsymbol{h}\} \tag{24}$$

and $\boldsymbol{x}$ is the first-stage decision variables representing the binary *buy/not buy* and *sell/not sell* decisions of every single MG, $\boldsymbol{y}$ is the second-stage variables representing the continuous operating decisions related to optimal power flow of the MMG, $\boldsymbol{d}$ denotes the uncertain power output of PV whose randomness is described by the uncertainty set $\mathbf{D}$.

In Eq. (21) collects constraints with only binary variables which describe the mutually exclusive relationships of buying/selling and charging/discharging status ((1), (2), (12) and (13)), whereas (22) denotes all constraints with only continuous variables ((7) and (11)), and Eq. (23) summarizes the power balance Eqs. (9), (10), (16), (17) and (24) represents constraints with both binary and continuous variables ((3)–(6), (8), (14), (15)).

4. Solution methodology

As mentioned above, the proposed two-stage adaptive robust optimization model not only materializes in multilevel optimization structure, but they are also strongly coupled to each other, which can easily cause NP-hard problems. Generally, two-stage models can be solved by cutting plane solution methods, such as Benders decomposition method [38] and its several extended methods [37,39]. Although such methods can exactly solve the problems with both continuous and binary variables, the increase in computational time with the problem size may weaken its solution capability on power system scheduling problems. Based on a different cutting plane strategy, a column-and-constraint generation (C&CG) algorithm is presented in [40] to solve two-stage robust optimization problems. C&CG has been proved to have better computational performance and stronger solution capability on two-stage RO problems in several areas, like power systems and energy systems[41–43]. Therefore, in this paper, we adopt C&CG algorithm to solve the proposed model. First, the two-stage adaptive robust model is decomposed into a master problem (MP) determining discrete transaction combinations and a subproblem (SP) optimizing continuous system operation. Then, MP and SP are solved iteratively with gradually identifying significant PV generation scenarios in SP and adding corresponding constraints with recourse variables into MP. Finally, the problem converges to an optimal solution within a small number of iterations. Moreover, the convergence proofs and related properties of C &CG is provided in [40,41].

For clarity, in this section, we use the compact format of the model given in Section 3.2 to introduce the model's transformation and solution procedures. The transformation of the detailed model is provided in Appendix B.

4.1. Master problem for energy transaction combinations

The master problem aims to obtain a solution of energy transaction decisions $\boldsymbol{x}$ which can withstand all uncertain scenarios of PV generation. By gradually identifying significant uncertain PV scenarios from SP at each iteration, corresponding constraints (27)–(30) are added to MP to cut the primal solution space until the optimal solution is derived. MP is formulated as follows.

$$\text{MP:} \quad \min_{\boldsymbol{x},\gamma} \quad \boldsymbol{a}^{\mathrm{T}}\boldsymbol{x} + \gamma \tag{25}$$

$$\text{s.t.} \quad \boldsymbol{C}\boldsymbol{x} \leqslant \boldsymbol{g}, \quad \boldsymbol{x} \in \{0,1\} \tag{26}$$

$$\gamma \geqslant \boldsymbol{b}^{\mathrm{T}}\boldsymbol{y}^{l}, \quad \forall\, l \leqslant k \tag{27}$$

$$\boldsymbol{E}\boldsymbol{y}^{l} \leqslant \boldsymbol{e}, \quad \forall\, l \leqslant k \tag{28}$$

$$\boldsymbol{A}\boldsymbol{y}^{l} + \boldsymbol{B}\boldsymbol{d}_{l}^{*} = \boldsymbol{c}, \quad \forall\, l \leqslant k \tag{29}$$

$$\boldsymbol{E}\boldsymbol{x} + \boldsymbol{F}\boldsymbol{y}^{l} = \boldsymbol{h}, \quad \forall\, l \leqslant k \tag{30}$$

where k is the iteration index, γ is the introduced auxiliary variable, operating decisions $\boldsymbol{y}^{l}$ are new recourse variables added into MP at the lth iteration of the algorithm. $\boldsymbol{d}_{l}^{*}$ denotes the optimal value of the uncertain parameter of PV generation obtained from SP at the lth iteration, thus it is considered fixed in MP. Note that MP is a MILP which can be directly solved by existing MIP solvers using Branch and Bound Method.

4.2. Subproblem for economic dispatch under uncertainty

For given energy transaction decisions $\boldsymbol{x}^*$ obtained from MP at each iteration, we solve the following subproblem to find the worst-case PV scenario $\boldsymbol{d}$ and the corresponding optimal power flow $\boldsymbol{y}$.

$$\text{SP:} \quad \max_{\boldsymbol{d}\in\mathbf{D}} \min_{\boldsymbol{y}\in\boldsymbol{\Omega}(\boldsymbol{x}^*,\boldsymbol{d})} \quad \boldsymbol{b}^{\mathrm{T}}\boldsymbol{y} \tag{31}$$

$$\text{s.t.} \quad \boldsymbol{E}\boldsymbol{y} \leqslant \boldsymbol{e} \tag{32}$$

$$\boldsymbol{A}\boldsymbol{y} + \boldsymbol{B}\boldsymbol{d} = \boldsymbol{c} \tag{33}$$

$$\boldsymbol{E}\boldsymbol{x}^* + \boldsymbol{F}\boldsymbol{y} \leqslant \boldsymbol{h} \tag{34}$$

Remark. When the inner program of a bi-level problem is linear, the inner-level problem can be equivalently transferred based on Karush-Kuhn-Tucker (KKT) optimality conditions [44] or strong duality theory [40].

Accordingly, the bi-level subproblem is converted into an equivalent single-level program by its KKT conditions as follows.

$$\text{KKT-SP:} \quad \max_{\substack{\boldsymbol{d}\in\mathbf{D}\\ \boldsymbol{y}\in\boldsymbol{\Omega}(\boldsymbol{x}^*,\boldsymbol{d})\\ \boldsymbol{\lambda},\boldsymbol{\mu},\boldsymbol{\omega}}} \quad \boldsymbol{b}^{\mathrm{T}}\boldsymbol{y} \tag{35}$$

s.t. (32)–(34)

$$\boldsymbol{E}^{\mathrm{T}}\boldsymbol{\lambda} + \boldsymbol{A}^{\mathrm{T}}\boldsymbol{\mu} + \boldsymbol{F}^{\mathrm{T}}\boldsymbol{\omega} = \boldsymbol{b} \tag{36}$$

$$(\boldsymbol{E}\boldsymbol{y}-\boldsymbol{e})_m\lambda_m = 0\,, \quad \forall\, m \tag{37}$$

$$(\boldsymbol{E}\boldsymbol{x}^* + \boldsymbol{F}\boldsymbol{y}-\boldsymbol{h})_n\omega_n = 0\,, \quad \forall\, n \tag{38}$$

$$(\boldsymbol{E}^{\mathrm{T}}\boldsymbol{\lambda} + \boldsymbol{A}^{\mathrm{T}}\boldsymbol{\mu} + \boldsymbol{F}^{\mathrm{T}}\boldsymbol{\omega}-\boldsymbol{b})_q y_q = 0\,, \quad \forall\, q \tag{39}$$

$$\boldsymbol{\lambda},\boldsymbol{\omega} \leqslant 0,\ \boldsymbol{\mu} \text{ is free} \tag{40}$$

where $\boldsymbol{\lambda},\boldsymbol{\mu},\boldsymbol{\omega}$ are dual variables for (32)–(34), respectively, and m,n,q are indices of constraints and variables. Constraints (37)–(39) are complementary slackness conditions which are nonlinear, and they can be linearised by using big-M method and introducing binary variables. The big-M method ensures the equality of terms only when a certain binary variable takes on one value, but leaves the terms "open" when the binary variable takes on its opposite value. Taking (37) as an example, it can be reformulated as follows.

$$\lambda_m \geqslant -\epsilon_m M, (\boldsymbol{E}\boldsymbol{y}-\boldsymbol{e})_m \geqslant -(1-\epsilon_m)M\,, \epsilon_m \in \{0,1\} \tag{41}$$

where M is a large enough constant. The constraints mean that, if $\epsilon_m = 0$, then $\lambda_m = 0$ and $\boldsymbol{E}\boldsymbol{y} \leqslant \boldsymbol{e}$, else if $\epsilon_m = 1$, then $\lambda_m \leqslant 0$ and $\boldsymbol{E}\boldsymbol{y} = \boldsymbol{e}$. Thus, it is equivalent to constraint (37).

So, KKT-SP is transformed into MILP and can be efficiently solved by existing MIP solvers.

4.3. C&CG algorithm

Based on the above master problem and subproblem, the procedures to solve the two-stage robust MMG operation problem are described in Fig. 3.

5. Case study

5.1. Input data

In this section, the proposed collaborative operation approach is implemented day-ahead in a residential community consisting of five heterogeneous house-level microgrids. The five users own the same roof-top PVs, different types of EVs and domestic loads. The load profiles of hourly data on a typical summer day for the five houses are shown in Fig. 4. The output profile of the 8 kWp PV unit on the same summer day is given in Fig. 5. For every house, the deviation from the predicted values of PV output is set to 0.5 kW. The exchanged power in each transaction is bound to 50 kW.

Considering the regular routines and travel time of residents, the PEVs are assumed to be plugged in for a period of 12 h every day from 20:00 every night to 8:00 the next morning, which is the common off-duty time of people. The types of PEVs in different houses are considered different. The relevant parameters are shown in Table 1[45]. The charging and discharging rate limits of each PEV are set to be the same value, the efficiencies of charging and discharging for each PEV are also assumed to be the same. Considering the lifespan of batteries in EVs, the SOC is confined to range between 20% and 85%. The users' desired SOC at 8:00 is set to 85%. The initial SOCs of PEVs at 20:00 are assumed to be diverse and given in Table 1.

The O&M cost of PVs is 0.03 CNY/kW h. The charging and discharging cost of PEVs is 0.08 CNY/kW h. Considering the electricity market operating modes in China, the pricing signal is fixed in this paper. The TOU electricity tariffs in the grid and in the MMG are shown in Table 2. The fixed service charge for electricity exchanging in the MMG is assumed to be 0.2 CNY each transaction, while that for electricity exchanging with the grid is assumed to be 0.3 CNY each transaction.

5.2. Results and discussions

5.2.1. Simulation environment and settings

The developed model is programmed and simulated in GAMS 22.2 using CPLEX10.0.1 [46] with an OPTCR of 0%. OPTCR is the relative gap between the best estimate and the optimal integer solution which determines the quality of the integer solution. In a linear model, OPTCR = 0 means global optimum is obtained. The convergence tolerance of the algorithm is set to 0.1.

5.2.2. Evaluation of the benefits of energy exchanging among MGs

In this subsection, a comparison between the proposed operation

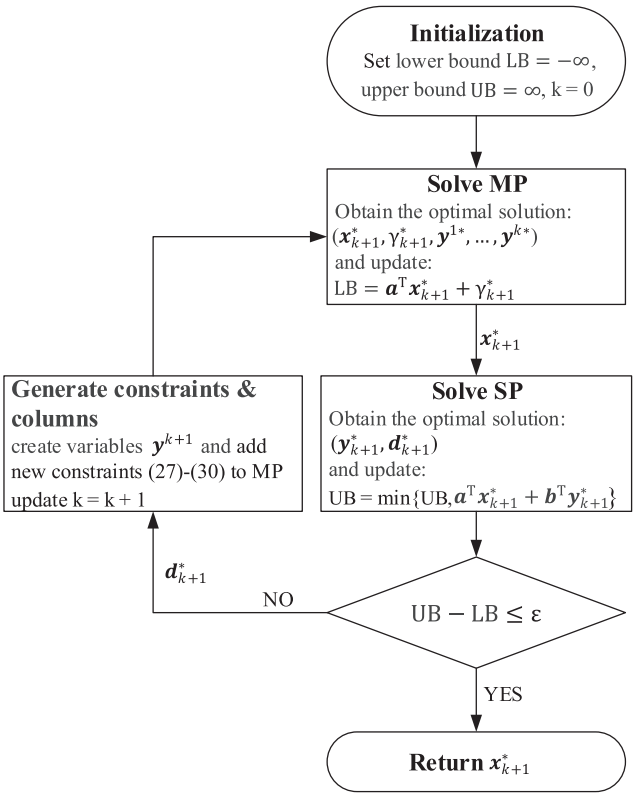

Fig. 3. The flow chart of C&CG algorithm.

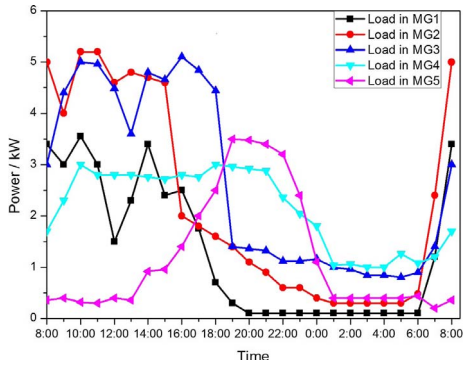

Fig. 4. Load profiles.

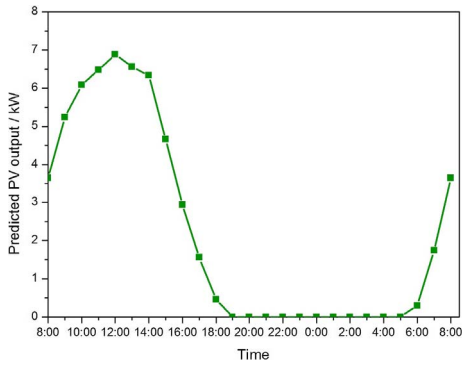

Fig. 5. The predicted PV output curve.

Table 1
Parameters of PEVs.

Index of PEVs	Battery capacity/ kW h	Charging & discharging rate limits/kW	Charging & discharging efficiencies	Initial values of SOC
PEV1	11.4	3	0.95	0.50
PEV2	10.0	3	0.94	0.33
PEV3	10.4	3	0.95	0.38
PEV4	13.8	3	0.96	0.40
PEV5	10.0	3	0.94	0.60

Table 2
Electricity tariffs (unit: CNY/kW h).

Time intervals	Purchasing price from the grid	Selling price to the grid	Exchanging price in the MMG
Peak (10:00–15:00, 18:00–21:00)	1.32	1.00	1.162
Flat (07:00–10:00, 15:00–18:00,21:00–23:00)	0.82	0.58	0.726
Valley (23:00–07:00)	0.33	0.20	0.260

model (ARO-Model) and Non-interactive Model (NI-Model) is presented, aiming to evaluate the performance of ARO-Model and the advantages of energy trading among MGs. As mentioned in Section 3, in NI-Model, MGs operate independently, so there is no energy exchange among MGs. Here, parameter *budget of uncertainty* for the PV unit is set to 3, which means the PV output might deviate from the forecasted profile in arbitrary three hours of the period when the PV unit has power output. Before solving ARO-Model, the values of parameters $cost_0(i)$ should be acquired. Therefore, NI-Model is solved first and the operating cost of each MG is calculated and assigned to $cost_0(i)$. The scheduling schemes for each MG under the two different models are shown in Fig. 6.

From Fig. 6, it can be seen that the scheduling results in ARO-Model are quite different from the ones in NI-Model. Here, we only take three time intervals (08:00–09:00, 16:00–17:00, 20:00–21:00) as examples to particularize their differences in power transactions.

During 08:00 and 09:00, the load demand in MG2 is more than its PV output while the load demand in MG5 is less than its PV output. In NI-Model, energy exchanging among MGs is not allowed and each MG is connected to the grid independently, so MG5 is scheduled to sell its excess power to the grid while MG2 needs to purchase power from the grid to supply its load demand. In contrast, under scheduling of ARO-Model model, MG2 is scheduled to purchase its needed 1.36 kW of power from MG5. Consequently, the system needn't buy power from and sell power to the grid simultaneously.

During 16:00 and 17:00, the PV generation in MG3 cannot meet its load demand, whereas MG5 has excessive power. Under NI-Model, MG5 feeds back to the grid while MG3 purchases power from the grid. In comparison, under ARO-Model, MG5 sells 2.16 kW of its surplus power to MG3, so both MG3 and MG5 needn't exchange power with the grid.

In 20:00–21:00, the peak period, EVs are plugged in and can be scheduled to supply the loads. At this time, the load in MG1 is only 0.1 kW, so MG1 can sell the stored energy of its EV besides its own demand supply. The load demand in MG5 is 3.48 kW, which is relatively big and cannot be fully supplied by its EV battery, so MG5 has to purchase power. Under NI-Model, MG1 sells the stored energy of its EV to the grid while MG5 purchases power from the grid, which leads to both high electricity cost and frequent power exchanging with the grid. In comparison, under ARO-Model, MG1 sells the discharged energy from its EV to MG5, so that the stored energy is first coordinated within the MMG to reduce the MMG's dependence on the grid and the total cost.

From the above observations, it can be concluded that energy exchanging among multiple MGs can facilitate the local coordination and consumption of renewable energy within the MMG, and thus reduce the amount and number of energy exchanging with the grid.

In addition, during 23:00–06:00, the night period, there is no generation from the PVs and loads are pretty small. Therefore, in most time intervals, the EV batteries are scheduled to discharge for demand supply. And in some other intervals, MGs purchase power from the grid to charge the EV batteries in order to achieve the desired SOC values at 08:00. So, there is no power exchange among MGs during 23:00–06:00.

Fig. 7 presents the amount of power exchange between the MMG and the grid in each hour under two models. There are three main observations from the results. Firstly, during daytime 08:00–17:00, the MMG mainly sells power to the grid in the optimal results of both models. But compared with NI-Model, the amount of sold power in ARO-Model is smaller in most of these hours, specifically, 1.36 kW smaller in 08:00–09:00, 1.26 kW smaller in 10:00–11:00, 0.04 kW smaller in 13:00–14:00, 0.5 kW smaller in 14:00–15:00, 2.16 kW smaller in 16:00–17:00, which means that power exchanging among MGs can mitigate the pressure of power exchanging on the grid. Secondly, during night 17:00–07:00, the MMG mainly purchases power from the grid under both models. But compared to NI-Model, in ARO-Model, the amount of purchased power during peak and flat period is smaller while the one during valley period (00:00–01:00, 03:00–04:00, 05:00–06:00) is greater, which shows that ARO-Model performs better in load shifting. Thirdly, it is observed that the MMG often buys power from and sells power to the grid simultaneously under NI-Model, such as the period 8:00–9:00, 16:00–17:00 and 20:00–21:00, whereas there is no such case happening in ARO-Model, which means ARO-Model can mitigate the pressure of frequent energy exchange on the grid through motivating local renewable energy consumption and also ensures the flexibility and security of the grid scheduling by managing the MMG as a whole.

In Fig. 8, (a) and (b) plot the different variation of five EV batteries' SOC in both models respectively. All the EVs discharge during the first few peak intervals (20:00–00:00) after they are plugged in their

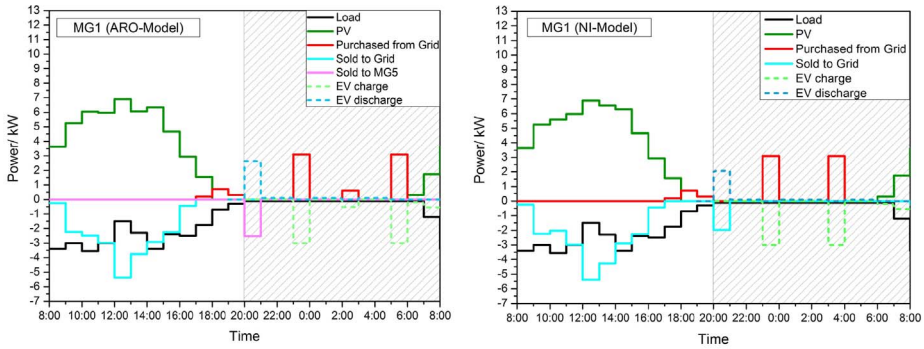

(a) Optimal scheduling results of MG1 in ARO-Model (b) Optimal scheduling results of MG1 in NI-Model

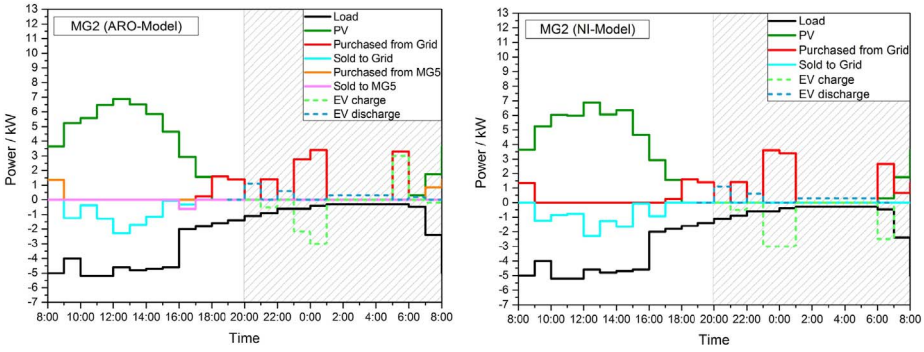

(c) Optimal scheduling results of MG2 in ARO-Model (d) Optimal scheduling results of MG2 in NI-Model

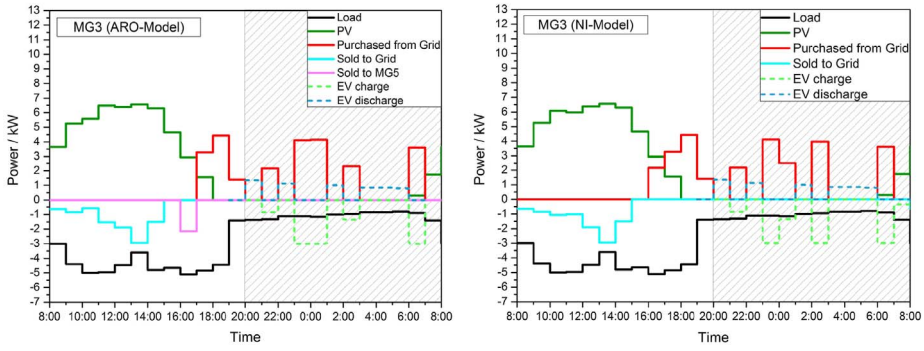

(e) Optimal scheduling results of MG3 in ARO-Model (f) Optimal scheduling results of MG3 in NI-Model

Fig. 6. Comparison of optimal scheduling results under different optimization models. (Note: The shadowed areas in the figures denote the period when EVs are plugged-in and schedulable.)

respective MGs. Then, during the next few valley intervals (00:00–08:00), they are scheduled to charge to reach the targeted SOC values or discharge to supply their own load demand. Moreover, although these EVs have different initial SOC values, all of them can achieve the desired SOC values set by their own users at 8:00 every morning when they depart, which suggests that ARO-Model performs well in properly scheduling EV batteries and satisfying users' requirements.

The MMG operating cost and each part of the cost in the two models are listed in Table 3. Compared to NI-Model, although energy exchange among MGs can incur some service cost, it also reduces the cost related to exchange with the grid by reducing the amount of electricity exchanged between the MMG and the grid, and note that the reduced cost is larger than the extra service cost. Meanwhile, because the costs related to EVs and PVs under ARO-Model are almost the same as those under NI-Model, the MMG operating cost is reduced in ARO-Model. In this case, ARO-Model saves 2.737 CNY of the MMG operating cost each day, which means the total cost is reduced by 18.05%. Thus, we can conclude energy exchange among MGs can help save the MMG operating cost.

5.2.3. *Adjustment of the conservatism of ARO-Model*

As mentioned in Section 3, the conservative level of ARO-Model can be controlled by adjusting $\Gamma(i)$. In this paper, $\Gamma(i)$ takes integer values. Since the PVs in our case have available output power only for 12 h during daytime, $\Gamma(i)$ takes a value from 0 to 12, in which $\Gamma(i) = 0$

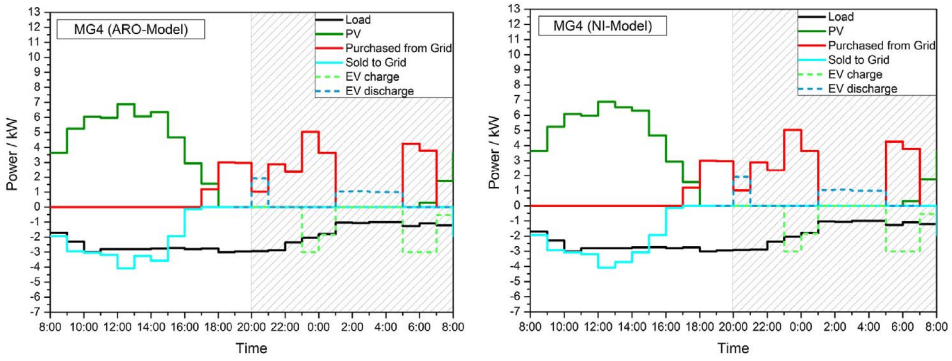

(g) Optimal scheduling results of MG4 in ARO-Model (h) Optimal scheduling results of MG4 in NI-Model

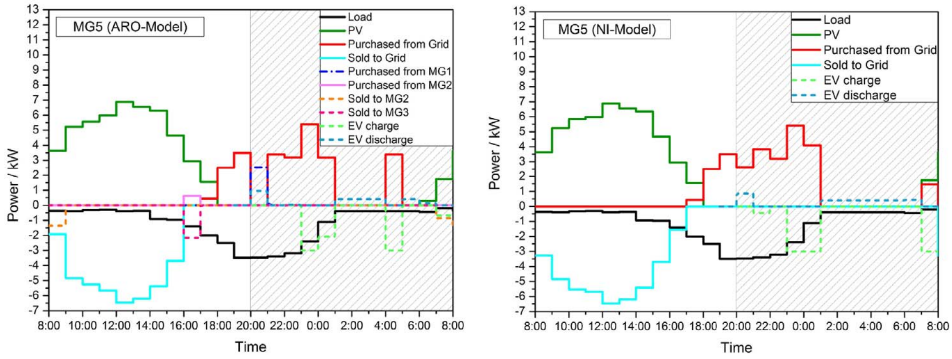

(i) Optimal scheduling results of MG5 in ARO-Model (j) Optimal scheduling results of MG5 in NI-Model

Fig. 6. (*continued*)

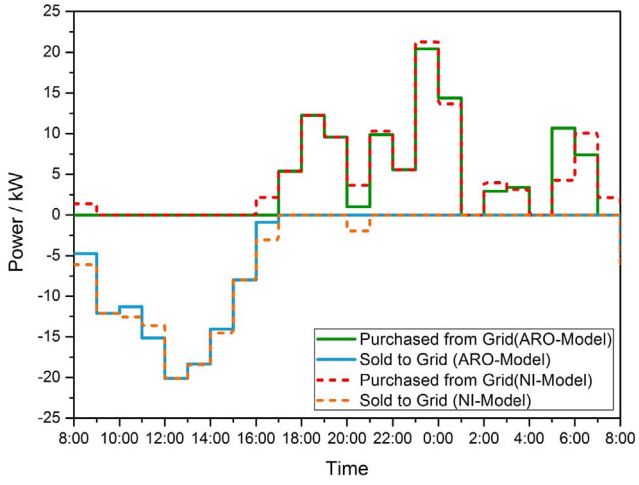

Fig. 7. Energy exchange between MMG and the grid.

implies that the PV forecast will not have mismatches in any time intervals and the model can be considered as the deterministic formulation.

In Table 4, the MMG operating cost obtained from Section 5.2.2 using ARO-Model is compared with that obtained using the deterministic formulation under the same uncertain PV scenario (here, the uncertain PV scenario means that the PV output might deviate from the predicted value in arbitrary three hours of the whole day). Under the deterministic case, uncertain PV output is not considered in the scheduling scheme, so additional cost will be produced as the penalty for extra energy supply or energy shortage. It is observed that the MMG operation cost is significantly lower in ARO-Model than the deterministic formulation. The result shows that, ARO-Model considers the worst case to hedges the MMG against PV uncertainty when making decisions, so it improves the economic benefits and robustness of MMG operation. Thus, it is necessary to consider uncertain factors in MMG optimization.

Table 5 presents the MMG operating costs under four different *budgets of uncertainty*. With the increase of $\Gamma(i)$, the uncertain level of PV becomes higher, which means PV output power is likely to become less. As presented in Table 6, as $\Gamma(i)$ becomes larger, the system is scheduled to purchase more electricity from the grid and sell less electricity to the grid in order to immunize against PV uncertainty, which causes the increase of the MMG operating cost. It can be concluded that higher *budget of uncertainty* leads to worse economic but better risk performance, namely a higher conservatism level of the model. Thus, in practical applications, operators can flexibly choose a suitable *budget of uncertainty* to adjust the robust scheduling and preciously describe the uncertainty in real-world scenarios.

5.2.4. Response to network dynamics

In this subsection, in order to show the response ability of our method to network dynamics, a simulation in which the MG number of the MMG changes is presented. In this scenario, there are three MGs (MG1, MG2, MG3) in the MMG for the first 8 h (08:00–16:00) of the day, then at 16:00, MG5 in the case study of Section 5.2.2 joins in the MMG for 8 h, finally at 00:00, MG5 quits the joint operation.

Firstly, the 24-h scheduling for the three-microgrid MMG is implemented, then at 16:00, MG5 joins and the remaining 16-h scheduling for the new four-microgrid MMG is implemented, finally at 00:00, MG5 quits the joint operation and the remaining 8-h scheduling for the three-microgrid MMG is implemented. Here, we give the simulation results of

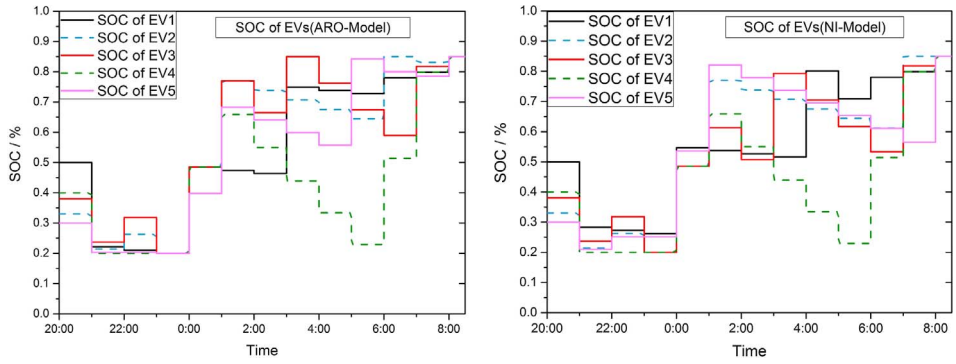

(a) SOC profiles in ARO-Model (b) SOC profiles in NI-Model

Fig. 8. EV batteries' SOC profiles of the five MGs.

Table 3
Operating cost of the MMG (unit: CNY).

Items	NI-Model	ARO-Model
Total cost related to exchange among MGs	0	2
Total cost related to exchange with the grid	1.913	−2.785
Total EVs' charging/discharging cost	5.545	5.506
Total O&M cost of PVs	7.707	7.707
MMG operating cost	15.165	12.428

Table 4
Comparative analysis of the system daily operation cost.

Approaches	MMG operating cost/CNY
Deterministic	14.918
ARO ($\Gamma(i) = 3$)	12.428 (−16.69%)

Table 5
MMG operating costs under different $\Gamma(i)$.

$\Gamma(i)$	3	6	9	12
MMG operating cost/CNY	12.428	19.668	24.023	27.037

Table 6
Model statistics for 5-MG MMG.

	Items	ARO-Model	NI-Model
Subproblem	No. of equations	11,430	3630
	No. of cont. variables	4590	1590
	No. of bin. variables	3420	1020
Master problem	No. of equations	5492	1647
	No. of cont. variables	1742	542
	No. of bin. variables	1680	480
Total	No. of iterations	2	3
	Computational time	960.53 s	180.37 s

MG1 to show the operation of MGs which are in the MMG during the whole process, and the results of MG5 to show the operation of the dynamic MG, as shown in Fig. 9.

The optimal solution of our proposed model can still be obtained even when the MMG meets network changes. As can be observed, the operation of those MGs which participate in the MMG operation for the whole 24 h are not influenced by the network changes brought by the joining of MG5. And MG5 can operate normally no matter when it joins in the MMG. In our approach, each MG is an independent entity, so adding new MGs or removing MGs do not have an impact on the operation of other MGs, MGs only have to decide which existing MGs to exchange energy with. Thus, we can conclude that joining new MGs or removing existing MGs do not bring big disturbances to the MMG, and our method can optimally schedule the MMG operation when network changes occur.

5.2.5. Computational analysis

As analyzed in Sections 2 and 3, the investigated MMG operation problem is considered as a large-scale robust unit commitment problem, in which not only the binary commitment decisions of MG exchange are considered, but the continuous operation of each MG is involved. Therefore, the formulated model is a large-scale two-stage robust optimization model including plenty of decision variables and constraints.

The computational information of ARO-Model in the last iteration from the case study in Section 5.2.2 is provided in Table 6. As can be observed, the size of the subproblem for economic dispatch under uncertainty is much larger than the master problem for energy transaction combinations. This is because a big number of dual variables are needed to formulate the KKT conditions and also a considerable number of binary variables are incorporated to linearize the bilinear products in the KKT conditions when transforming the bi-level subproblem to a single-level problem. Thus, in each iteration, the subproblem presents more computational challenges than the master problem. Totally, the algorithm only needs 2 iterations to converge to the optimal solutions in a reasonable time of 960.53 s. And in any cases, for the studied five-microgrid MMG, the number of iterations is no more than three and the individual computational time never exceeds 1020 s (17 min), which suggests that C&CG can be implemented to efficiently solve the studied MMG operation problem.

In addition, the computational information of NI-Model is also shown in Table 6. It is observed that, both the constraints and variables in ARO-Model are three times more than the ones in NI-Model for both subproblem and master problem. This result suggests that, for the same MMG, energy transactions among MGs significantly increase the complexity of the MMG operation problem by adding constraints and variables related to the coordination of multiple MGs. And it also indicates that the selected algorithm is suitable for solving the proposed model.

The computational information of MMGs consisting of 3 MGs, 5 MGs, and 10 MGs are reported in Table 7. As can be observed, only two or three iterations are needed to solve these large-scale systems. As we increase the number of MGs in the MMG, the sizes of both subproblem and master problem increase, which means the problem complexity increases. The increase of the MMG scale leads to the multiplication of complexity of energy exchange among MGs, including the increase of commitment decisions in master problem and operation decisions in subproblem. The computational time also increases, but for the ten-microgrid MMG, the computational time is still in a reasonable range,

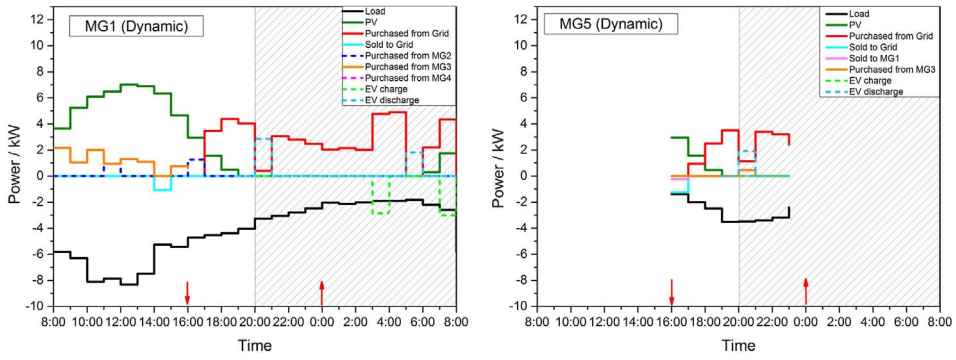

(a) Optimal scheduling results of MG1 when dynamics occur

(b) Optimal scheduling results of MG5 when dynamics occur

Fig. 9. Optimal scheduling results when network dynamics occur.

Table 7
Model statistics for MMGs of different scales.

	Items	3 MGs	5 MGs	10 MGs
Subproblem	No. of equations	4996	11,430	38,195
	No. of cont. variables	2044	4590	14,915
	No. of bin. variables	1476	3420	12,120
Master problem	No. of equations	3884	5492	18,147
	No. of cont. variables	758	1742	5882
	No. of bin. variables	720	1680	5760
Total	No. of iterations	3	2	2
	Computational time	34.72 s	960.53 s	2012.35 s

which needs about 33 min.

6. Conclusions

In this paper, the MMG energy transaction coordination and economic operation problem under uncertainty is studied. To explicitly model the energy interactive behaviours among multiple MGs from the system-level perspective, the problem is treated as unit commitment problem, which is more suitable for large-scale multi-stage problems. Thus, a two-stage adaptive robust optimization formulation is developed to minimize the total MMG operating cost, of which the first-stage is to make *buy/sell* decisions for MGs and the second-stage is to optimize the power to be purchased/sold under the worst-case PV scenarios.

Numerical results show that, compared with NI-Model without energy exchange among MGs, the daily MMG operating cost under the proposed ARO-Model is reduced by about 18.05%, the number of energy exchange between the MMG and the grid under reduces from 25 to 21 during 24 h, which is decreased by 16%, and the total amount of energy exchange including purchasing and selling is decreased by 5.30%, in addition, the case that the MMG imports electricity from and exports electricity to the grid simultaneously is mitigated. The results demonstrate that energy transactions in the MMG can improve its economic performance by encouraging local energy consumptions and alleviate its impact on the grid by making its exchange with the grid more orderly. Compared with the deterministic model, the results indicate that the proposed model can diminish the cost increase caused by uncertainty and also allows adjusting conservatism level of uncertainty according to the real-world application scenarios. Simulation results also show that the proposed approach can response to network dynamics and optimize the MMG operation normally. Moreover, the computational analysis shows that C&CG algorithm can be successfully used to solve a MMG operation optimization problem in a few iteration times. The proposed model can be employed in centralized MMG energy management system to provide optimal guidance for energy interactive behaviours among MGs and improve the MMG energy efficiency.

The proposed approach is a meaningful attempt for scheduling residential MMGs. The results obtained reveal that this scheduling approach could be properly integrated into the aggregator's optimizer by the scheduling software. Here, the optimizer can accept and transmit the external information such as electricity prices and load forecasting. Then, the information are used as input data of the scheduling software to calculate the optimal energy scheduling scheme, which is actually control set-point values including the charge/discharge status of PEVs and the amount of power. Finally, the set-point values are sent to the I-box of each MG to perform control actions. Therefore, the proposed approach could be used for real applications to assist MMG operators on their decision making and facilitate the joint operation of multiple MGs in a local district. Furthermore, besides MGs with PVs, the method developed in our work can also be generalized to the optimization problem of MMGs containing a variety of distributed generation sources.

There are some limitations of this study, which need to be further studied in our future work. First, the energy price is assumed to be fixed in this paper. Although fixed tariff is the current electricity market mode in China, dynamic tariffs might motivate MGs to more actively participate in MMG energy transaction through appropriate market mechanisms, such as Cournot Nash pricing mechanism [47]. Second, stochastic behaviours of PEV users are neglected. Although the selected PEV pattern in case studies corresponds to general behaviours of residential users, there exist many uncertain factors which would influence operation decisions and should be fully considered, such as using big data analytics to characterize PEV behaviours [48].

Acknowledgements

This work is supported by Shandong Provincial Natural Science Foundation – China (Grant No. ZR2014FM036).

Appendix A. NI-Model

The difference between NI-Model and ARO-Model in this paper is that the energy exchange among MGs is not allowed in NI-Model. Thus, in NI-Model, the terms in objective function and constraint (10) as well as constraints (1), (3), (4), (7), (8) which are related to energy exchange among MGs are deleted. The other Constraints are the same as Section 3 and thus are omitted here.

The objective function (42) is to minimize the MMG operation cost, which involves the following terms: the cost associated with electricity exchanging which includes both the fixed service charge of the aggregator and the electricity cost, the operation and maintenance (O&M) cost of PVs, the charging and discharging cost of EVs' batteries.

The complete NI-Model is formulated in the following.

$$TC = \min_{\substack{\boldsymbol{u},\boldsymbol{v}\\ \boldsymbol{z},\boldsymbol{w}}} \sum_{t=0}^{23}\sum_{i=1}^{n} (u(i,t)b_{ser} + v(i,t)b_{ser}) + \max_{\mathbf{U}}\min_{\boldsymbol{\Omega}_0} \sum_{t=0}^{23}\sum_{i=1}^{n} (p_{pv}(i,t)C_{pv}(i) + (p_{ec}(i,t) + p_{ed}(i,t))C_{ev}(i) + p_{gb}(i,t)c_{gb}(t) - p_{gs}(i,t)c_{gs}(t)) \tag{42}$$

s.t.

(2)(12)(13)

where

$\boldsymbol{\Omega}_0(\boldsymbol{u},\boldsymbol{v},\boldsymbol{z},\boldsymbol{w},\boldsymbol{p}_{pv}) = \{(\boldsymbol{p}_{ec},\boldsymbol{p}_{ed},\boldsymbol{p}_{gb},\boldsymbol{p}_{gs},\boldsymbol{SOC}_{ev})$:(5),(6),(9),(11),(14)-(17),(43)},

and **U** is the same as in Section 3.

The terms related to exchange among MGs in (10) are deleted, so the constraint of power balance of MG i is as follows.

$$P_l(i,t) + p_{ec}(i,t) + p_{gs}(i,t) = p_{pv}(i,t) + p_{ec}(i,t) + p_{gb}(i,t)\,, \quad \forall\, i,j \in G\,, \quad \forall\, t \in T \tag{43}$$

Appendix B. Transformation of ARO-Model

MP:

$$TC = \min_{\substack{\boldsymbol{r},\boldsymbol{s},\boldsymbol{u}\\ \boldsymbol{v},\boldsymbol{z},\boldsymbol{w}}} \sum_{t=0}^{23}\sum_{i=1}^{n} \left(\sum_{j=1,j\neq i}^{n} (r(i,j,t)a_{ser} + s(i,j,t)a_{ser}) + u(i,t)b_{ser} + v(i,t)b_{ser} \right) + \eta_0 \tag{44}$$

s.t.

(1)(2)(12)(13)

$$\eta_0 \geqslant \sum_{t=0}^{23}\sum_{i=1}^{n} (p^*_{pv,l}(i,t)C_{pv}(i) + (p^l_{ec}(i,t) + p^l_{ed}(i,t))C_{ev}(i) + p^l_{gb}(i,t)c_{gb}(t) - p^l_{gs}(i,t)c_{gs}(t))\,, \quad \forall\, l \leqslant k \tag{45}$$

$$0 \leqslant p^l_{mb}(i,j,t) \leqslant r(i,j,t)P^{max}_m\,, \quad \forall\, i,j \in G,\ \ j \neq i\,, \quad \forall\, t \in T\,, \quad \forall\, l \leqslant k \tag{46}$$

$$0 \leqslant p^l_{ms}(i,j,t) \leqslant s(i,j,t)P^{max}_m\,, \quad \forall\, i,j \in G,\ \ j \neq i\,, \quad \forall\, t \in T\,, \quad \forall\, l \leqslant k \tag{47}$$

$$0 \leqslant p^l_{gb}(i,t) \leqslant u(i,t)P^{max}_{gb}\,, \quad \forall\, i \in G\,, \quad \forall\, t \in T\,, \quad \forall\, l \leqslant k \tag{48}$$

$$0 \leqslant p^l_{gs}(i,t) \leqslant v(i,t)P^{max}_{gs}\,, \quad \forall\, i \in G\,, \quad \forall\, t \in T\,, \quad \forall\, l \leqslant k \tag{49}$$

$$p^l_{mb}(i,j,t) = p^l_{ms}(j,i,t)\,, \quad \forall\, i,j \in G,\ \ j \neq i\,, \quad \forall\, t \in T\,, \quad \forall\, l \leqslant k \tag{50}$$

$$\sum_{t=0}^{23}\sum_{j=1,j\neq i}^{n} (r(i,j,t) + s(i,j,t))a_{ser} + \sum_{t=0}^{23} (u(i,t) + v(i,t))b_{ser} + \sum_{t=0}^{23} p^*_{pv,l}(i,t)C_{pv}(i) + \sum_{t=0}^{23} (p^l_{ec}(i,t) + p^l_{ed}(i,t))C_{ev}(i) + \sum_{t=0}^{23}\sum_{j=1,j\neq i}^{n} (p^l_{mb}(i,j,t) - p^l_{ms}(i,j,t))c_m(t)$$
$$+ \sum_{t=0}^{23} (p^l_{gb}(i,t)c_{gb}(t) - p^l_{gs}(i,t)c_{gs}(t)) \leqslant cost_0(i)\,, \quad \forall\, i \in G\,, \quad \forall\, t \in T\,, \quad \forall\, l \leqslant k \tag{51}$$

$$\sum_{i=1}^{n} P_l(i,t) + \sum_{i=1}^{n} p^l_{ec}(i,t) + \sum_{i=1}^{n} p^l_{gs}(i,t) = \sum_{i=1}^{n} p^*_{pv,l}(i,t) + \sum_{i=1}^{n} p^l_{ed}(i,t) + \sum_{i=1}^{n} p^l_{gb}(i,t)\,, \quad \forall\, i \in G\,, \quad \forall\, t \in T\,, \quad \forall\, l \leqslant k \tag{52}$$

$$P_{load}(i,t) + p^l_{ec}(i,t) + \sum_{j=1,j\neq i}^{n} p^l_{ms}(i,j,t) + p^l_{gs}(i,t) = p^*_{pv,l}(i,t) + p^l_{ed}(i,t) + \sum_{j=1,j\neq i}^{n} p^l_{mb}(i,j,t) + p^l_{gb}(i,t)\,, \quad \forall\, i,j \in G\,, \quad \forall\, t \in T\,, \quad \forall\, l \leqslant k \tag{53}$$

$$SOC^{min}_{ev}(i) \leqslant SOC^l_{ev}(i,t) \leqslant SOC^{max}_{ev}(i)\,, \quad \forall\, i \in G\,, \quad \forall\, t \in T\,, \quad \forall\, l \leqslant k \tag{54}$$

$$0 \leqslant p^l_{ec}(i,t) \leqslant z(i,t)P^{max}_{ec}(i)\,, \quad \forall\, i \in G\,, \quad \forall\, t \in T\,, \quad \forall\, l \leqslant k \tag{55}$$

$$0 \leqslant p^l_{ed}(i,t) \leqslant w(i,t)P^{max}_{ed}(i)\,, \quad \forall\, i \in G\,, \quad \forall\, t \in T\,, \quad \forall\, l \leqslant k \tag{56}$$

$$SOC^l_{ev}(i,t+1)Cap_{ev}(i) = SOC^l_{ev}(i,t)Cap_{ev}(i) + \eta_{ec}(i)p^l_{ec}(i,t)\Delta_T - \frac{1}{\eta_{ed}(i)}p^l_{ed}(i,t)\Delta_T\,, \quad \forall\, i \in G\,, \quad \forall\, t \in T_P\,, \quad \forall\, l \leqslant k \tag{57}$$

$$SOC_{ev}(i,t_1)Cap_{ev}(i) + \sum_{t=t_1}^{t_2-1} \left(\eta_{ec}(i)p^l_{ec}(i,t)\Delta_T - \frac{1}{\eta_{ed}(i)}p^l_{ed}(i,t)\Delta_T \right) = SOC_{ev}(i,t_2)Cap_{ev}(i)\,, \quad \forall\, i \in G\,, \quad \forall\, t \in T_P\,, \quad \forall\, l \leqslant k \tag{58}$$

SP:

The bi-level subproblem **SP** is omitted here and its equivalent formulation **KKT-SP** transformed by KKT conditions is given in the following.

Theorem 1. *Problem* **SP** *has an equivalent MILP formulation as* **KKT-SP**.

Proof. The inner *min* problem of bi-level **SP** is a linear program, so its optimal solutions can be represented by its KKT conditions, which include its primal constraints, dual constraints and complementary slackness constraints. Therefore, **SP** is equivalently converted to the single-level optimization model as follows:

KKT-SP:

$$\max_{\mathbf{U},\Omega} \sum_{t=0}^{23} \sum_{i=1}^{n} (p_{pv}(i,t)C_{pv}(i) + (p_{ec}(i,t) + p_{ed}(i,t))C_{ev}(i) + p_{gb}(i,t)c_{gb}(t) - p_{gs}(i,t)c_{gs}(t)) \tag{59}$$

s.t.

Primal constraints:

(3)-(7),(9)-(11),(14)-(17)

Dual constraints:

Let $\pi_1(t),\pi_2(i,t)$ be dual variables for constraint (9), (10), $\pi_3(i,j,t)$ for constraint (7), $\pi_4(i,j,t),\pi_5(i,j,t),\pi_6(i,t),\pi_7(i,t)$ for constraint (3)–(6), $\pi_8(i,t)$ and $\pi_9(i,t)$ be dual variables for constraint (11) which actually represents two inequalities, $\pi_{10}(i,t),\pi_{11}(i,t),\pi_{12}(i,t),\pi_{13}(i)$ for constraint (14)–(17) individually.

$$\pi_1(t) + \pi_2(i,t) + \pi_{10}(i,t) - \eta_{ec}(i)\pi_{12}(i,t) - \eta_{ec}(i)\pi_{13}(i) \leqslant C_{ev}(i)\,, \quad \forall\, i \in G\,, \quad \forall\, t \in T_P \tag{60}$$

$$-\pi_1(t) - \pi_2(i,t) + \pi_{11}(i,t) + \frac{1}{\eta_{ed}(i)}\pi_{12}(i,t) + \frac{1}{\eta_{ed}(i)}\pi_{13}(i) \leqslant C_{ev}(i)\,, \quad \forall\, i \in G\,, \quad \forall\, t \in T_P \tag{61}$$

$$-\pi_2(i,t) + \pi_3(i,j,t) + \pi_4(i,j,t) \leqslant c_m(t)\,, \quad \forall\, i,j \in G,\ \ j \neq i\,, \quad \forall\, t \in T \tag{62}$$

$$\pi_2(i,t) - \pi_3(i,j,t) + \pi_5(i,j,t) \leqslant -c_m(t)\,, \quad \forall\, i,j \in G,\ \ j \neq i\,, \quad \forall\, t \in T \tag{63}$$

$$-\pi_1(t) - \pi_2(i,t) + \pi_6(i,t) \leqslant c_{gb}(t)\,, \quad \forall\, i \in G\,, \quad \forall\, t \in T \tag{64}$$

$$\pi_1(t) + \pi_2(i,t) + \pi_7(i,t) \leqslant -c_{gs}(t)\,, \quad \forall\, i \in G\,, \quad \forall\, t \in T \tag{65}$$

$$\pi_8(i,t_1) + \pi_9(i,t_1) - Cap_{ev}(i)\pi_{12}(i,t_1) \leqslant 0\,, \quad \forall\, i \in G,\ \ t = t_1 \tag{66}$$

$$\pi_8(i,t) + \pi_9(i,t) + Cap_{ev}(i)\pi_{12}(i,t-1) - Cap_{ev}(i)\pi_{12}(i,t) \leqslant 0\,, \quad \forall\, i \in G,\ \ t = t_1+1, t_1+2, \ldots, t_2-2 \tag{67}$$

$$\pi_8(i,t_2-1) + \pi_9(i,t_2-1) + Cap_{ev}(i)\pi_{12}(i,t_2-1) + \pi_{13}(i) \leqslant 0\,, \quad \forall\, i \in G,\ \ t = t_2-1 \tag{68}$$

Complementary slackness constraints:

$$\pi_4(i,j,t)(p_{mb}(i,j,t) - r(i,j,t)P_m^{max}) = 0\,, \quad \forall\, i,j \in G,\ \ j \neq i\,, \quad \forall\, t \in T \tag{69}$$

$$\pi_5(i,j,t)(p_{ms}(i,j,t) - s(i,j,t)P_m^{max}) = 0\,, \quad \forall\, i,j \in G,\ \ j \neq i\,, \quad \forall\, t \in T \tag{70}$$

$$\pi_6(i,t)(p_{gb}(i,t) - u(i,t)P_{gb}^{max}) = 0\,, \quad \forall\, i \in G\,, \quad \forall\, t \in T \tag{71}$$

$$\pi_7(i,t)(p_{gs}(i,t) - v(i,t)P_{gs}^{max}) = 0\,, \quad \forall\, i \in G\,, \quad \forall\, t \in T \tag{72}$$

$$\pi_8(i,t)(SOC_{ev}(i,t) - SOC_{ev}^{max}(i)) = 0\,, \quad \forall\, i \in G\,, \quad \forall\, t \in T \tag{73}$$

$$\pi_9(i,t)(SOC_{ev}(i,t) - SOC_{ev}^{min}(i)) = 0\,, \quad \forall\, i \in G\,, \quad \forall\, t \in T \tag{74}$$

$$\pi_{10}(i,t)(p_{ec}(i,t) - z(i,t)P_{ec}^{max}(i)) = 0\,, \quad \forall\, i \in G\,, \quad \forall\, t \in T \tag{75}$$

$$\pi_{11}(i,t)(p_{ed}(i,t) - w(i,t)P_{ed}^{max}(i)) = 0\,, \quad \forall\, i \in G\,, \quad \forall\, t \in T \tag{76}$$

$$p_{ec}(i,t)(\pi_1(t) + \pi_2(i,t) + \pi_{10}(i,t) - \eta_{ec}(i)\pi_{12}(i,t) - \eta_{ec}(i)\pi_{13}(i) - C_{ev}(i)) = 0\,, \quad \forall\, i \in G\,, \quad \forall\, t \in T_P \tag{77}$$

$$p_{ed}(i,t)\left(-\pi_1(t) - \pi_2(i,t) + \pi_{11}(i,t) + \frac{1}{\eta_{ed}(i)}\pi_{12}(i,t) + \frac{1}{\eta_{ed}(i)}\pi_{13}(i) - C_{ev}(i)\right) = 0\,, \quad \forall\, i \in G\,, \quad \forall\, t \in T_P \tag{78}$$

$$p_{mb}(i,j,t)(-\pi_2(i,t) + \pi_3(i,j,t) + \pi_4(i,j,t) - c_m(t)) = 0\,, \quad \forall\, i,j \in G,\ \ j \neq i\,, \quad \forall\, t \in T \tag{79}$$

$$p_{ms}(i,j,t)(\pi_2(i,t) - \pi_3(i,j,t) + \pi_5(i,j,t) + c_m(t)) = 0\,, \quad \forall\, i,j \in G,\ \ j \neq i\,, \quad \forall\, t \in T \tag{80}$$

$$p_{gb}(i,t)(-\pi_1(t) - \pi_2(i,t) + \pi_6(i,t) - c_{gb}(t)) = 0\,, \quad \forall\, i \in G\,, \quad \forall\, t \in T \tag{81}$$

$$p_{gs}(i,t)(\pi_1(t) + \pi_2(i,t) + \pi_7(i,t) + c_{gs}(t)) = 0\,, \quad \forall\, i \in G\,, \quad \forall\, t \in T \tag{82}$$

$$SOC_{ev}(i,t_1)(\pi_8(i,t_1) + \pi_9(i,t_1) - Cap_{ev}(i)\pi_{12}(i,t_1)) = 0\,, \quad \forall\, i \in G,\ \ t = t_1 \tag{83}$$

$$SOC_{ev}(i,t)(\pi_8(i,t) + \pi_9(i,t) + Cap_{ev}(i)\pi_{12}(i,t-1) - Cap_{ev}(i)\pi_{12}(i,t)) = 0\,, \quad \forall\, i \in G,\ \ t = t_1+1, t_1+2, \ldots, t_2-2 \tag{84}$$

$$SOC_{ev}(i,t_2)(\pi_8(i,t_2-1) + \pi_9(i,t_2-1) + Cap_{ev}(i)\pi_{12}(i,t_2-1)) = 0\,, \quad \forall\, i \in G,\ \ t = t_2-1 \tag{85}$$

Sign constraints:

$$\pi_4(i,j,t),\pi_5(i,j,t),\pi_6(i,t),\pi_7(i,t),\pi_8(i,t),\pi_{10}(i,t),\pi_{11}(i,t) \leqslant 0\ ,\quad \forall\ i \in G\ ,\quad \forall\ t \in T \tag{86}$$

$$\pi_9(i,t) \geqslant 0\ ,\quad \forall\ i \in G\ ,\quad \forall\ t \in T \tag{87}$$

$$\pi_1(t),\pi_2(i,t),\pi_3(i,j,t),\pi_{12}(i,t),\pi_{13}(i) \text{ are free},\quad \forall\ i \in G\ ,\quad \forall\ t \in T \tag{88}$$

Next, the nonlinear complementary slackness constraints (69)–(85) can be linearised using big-M method. Thus, we introduce a set of binary variables. Because the transformation for each constraint is similar, here, we only take the transformation for constraint (69) as an example. With Introduced binary variable $\lambda_4(i,j,t)$, constraint (69) can be replaced by

$$\pi_4(i,j,t) \geqslant -M(1-\lambda_4(i,j,t)),(p_{mb}(i,j,t)-r(i,j,t)P_m^{max}) \geqslant -M\lambda_4(i,j,t),\lambda_4(i,j,t) \in 0,1\ ,\quad \forall\ i,j \in G,\quad j \neq i\ ,\quad \forall\ t \in T \tag{89}$$

where M is a sufficiently large constant. By applying this conversion to each complementary slackness constraint, the whole **SP** is finally reformulated into a MILP problem **KKT-SP**. □

References

[1] Fathima AH, Palanisamy K. Optimization in microgrids with hybrid energy systems – a review. Renew Sustain Energy Rev 2015;45:431–46.
[2] Adefarati T, Bansal RC. Reliability and economic assessment of a microgrid power system with the integration of renewable energy resources. Appl Energy 2017;206:911–33.
[3] Jin M, Feng W, Liu P, Marnay C, Spanos C. MOD-DR: microgrid optimal dispatch with demand response. Appl Energy 2017;187:758–76.
[4] Al Faruque MA. RAMP: impact of rule based aggregator business model for residential microgrid of prosumers including distributed energy resources. In: Innovative smart grid technologies conference; 2014. p. 1–6.
[5] Kam MVD, Sark WV. Smart charging of electric vehicles with photovoltaic power and vehicle-to-grid technology in a microgrid; a case study. Appl Energy 2015;152:20–30.
[6] Wu P, Huang W, Tai N, Liang S. A novel design of architecture and control for multiple microgrids with hybrid AC/DC connection. Appl Energy 2018;210:1002–16.
[7] Ren L, Qin Y, Li Y, Zhang P, Wang B, Luh PB, et al. Enabling resilient distributed power sharing in networked microgrids through software defined networking. Appl Energy 2018;210:1251–65.
[8] Wang X, Wang C, Xu T, Guo L, Li P, Yu L, et al. Optimal voltage regulation for distribution networks with multi-microgrids. Appl Energy 2018;210:1027–36.
[9] Li P, Guan X, Wu J, Wang D. An integrated energy exchange scheduling and pricing strategy for multi-microgrid system. In: Tencon 2013 – 2013 IEEE region 10 conference; 2013. p. 1–5.
[10] Wang D, Guan X, Wu J, Li P, Zan P, Xu H. Integrated energy exchange scheduling for multimicrogrid system with electric vehicles. IEEE Trans Smart Grid 2016;7(4):1762–74.
[11] Chiu WY, Sun H, Poor HV. A multiobjective approach to multimicrogrid system design. IEEE Trans Smart Grid 2015;6(5):2263–72.
[12] Wang Z, Chen B, Wang J, Begovic MM, Chen C. Coordinated energy management of networked microgrids in distribution systems. IEEE Trans Smart Grid 2015;6(1):45–53.
[13] Wang Z, Chen B, Wang J, Kim J. Decentralized energy management system for networked microgrids in grid-connected and islanded modes. IEEE Trans Smart Grid 2016;7(2):1097–105.
[14] Kou P, Liang D, Gao L. Distributed EMPC of multiple microgrids for coordinated stochastic energy management. Appl Energy 2017;185:939–52.
[15] Xiao F, Ai Q. New modeling framework considering economy, uncertainty, and security for estimating the dynamic interchange capability of multi-microgrids. Electr Power Syst Res 2017;152:237–48.
[16] Hu M, Weir JD, Wu T. Decentralized operation strategies for an integrated building energy system using a memetic algorithm. Eur J Oper Res 2012;217(1):185–97.
[17] Hu M, Weir JD, Wu T. An augmented multi-objective particle swarm optimizer for building cluster operation decisions. Appl Soft Comput 2014;25(C):347–59.
[18] Nikmehr N, Najafi-Ravadanegh S. A study on optimal power sharing in interconnected microgrids under uncertainty. Int Trans Electr Energy Syst 2016;26(1):208–32.
[19] Nikmehr N, Najafi-Ravadanegh S, Khodaei A. Probabilistic optimal scheduling of networked microgrids considering time-based demand response programs under uncertainty. Appl Energy 2017;198:267–79.
[20] Asimakopoulou GE, Dimeas AL, Hatziargyriou ND. Leader-follower strategies for energy management of multi-microgrids. IEEE Trans Smart Grid 2013;4(4):1909–16.
[21] Ma L, Liu N, Wang L, Zhang J, Lei J, Zeng Z, et al. Multi-party energy management for smart building cluster with PV systems using automatic demand response. Energy Build 2016;121:11–21.
[22] Fathi M, Bevrani H. Statistical cooperative power dispatching in interconnected microgrids. IEEE Trans Sustain Energy 2013;4(3):586–93.
[23] Gregoratti D, Matamoros J. Distributed energy trading: the multiple-microgrid case. IEEE Trans Ind Electron 2015;62(4):2551–9.
[24] Xu Z, Hu G, Spanos CJ. Coordinated optimization of multiple buildings with a fair price mechanism for energy exchange. Energy Build 2017;151:132–45.
[25] Lv T, Ai Q. Interactive energy management of networked microgrids-based active distribution system considering large-scale integration of renewable energy resources. Appl Energy 2016;163:408–22.
[26] Wang Z, Chen B, Wang J, Chen C. Networked microgrids for self-healing power systems. IEEE Trans Smart Grid 2015;7(1):310–9.
[27] Hu M. A data-driven feed-forward decision framework for building clusters operation under uncertainty. Appl Energy 2015;141:229–37.
[28] Nikmehr N, Najafi-Ravadanegh S. Optimal power dispatch of multi-microgrids at future smart distribution grids. IEEE Trans Smart Grid 2015;6(4):1648–57.
[29] Haddadian H, Noroozian R. Multi-microgrids approach for design and operation of future distribution networks based on novel technical indices. Appl Energy 2017;185:650–63.
[30] Bertsimas D, Sim M. The price of robustness. Oper Res 2004;52(1):35–53.
[31] Kuznetsova E, Li YF, Ruiz C, Zio E. An integrated framework of agent-based modelling and robust optimization for microgrid energy management. Appl Energy 2014;129:70–88.
[32] Gupta RA, Gupta NK. A robust optimization based approach for microgrid operation in deregulated environment. Energy Convers Manage 2015;93:121–31.
[33] Wang L, Li Q, Ding R, Sun M, Wang G. Integrated scheduling of energy supply and demand in microgrids under uncertainty: a robust multi-objective optimization approach. Energy 2017;130:1–14.
[34] An Y, Zeng B. Exploring the modeling capacity of two-stage robust optimization: variants of robust unit commitment model. IEEE Trans Power Syst 2015;30(1):109–22.
[35] Ruiz C, Conejo AJ. Robust transmission expansion planning. Eur J Oper Res 2015;242(2):390–401.
[36] Bertsimas D, Gupta V, Kallus N. Data-driven robust optimization. Math Program 2017. http://dx.doi.org/10.1007/s10107-017-1125-8.
[37] Bertsimas D, Litvinov E, Sun XA, Zhao J, Zheng T. Adaptive robust optimization for the security constrained unit commitment problem. IEEE Trans Power Syst 2013;28(1):52–63.
[38] Jiang R, Wang J, Zhang M, Guan Y. Two-stage minimax regret robust unit commitment. IEEE Trans Power Syst 2013;28(3):2271–82.
[39] Jabr RA. Robust transmission network expansion planning with uncertain renewable generation and loads. IEEE Trans Power Syst 2013;28(4):4558–67.
[40] Zeng B, Zhao L. Solving two-stage robust optimization problems using a column-and-constraint generation method. Oper Res Lett 2013;41(5):457–61.
[41] Zhao L, Zeng B. Robust unit commitment problem with demand response and wind energy. In: Power and energy society general meeting; 2012. p. 1–8.
[42] Hu B, Wu L. Robust SCUC considering continuous/discrete uncertainties and quick-start units: a two-stage robust optimization with mixed-integer recourse. IEEE Trans Power Syst 2016;31(2):1407–19.
[43] Wang C, Jiao B, Guo L, Tian Z, Niu J, Li S. Robust scheduling of building energy system under uncertainty. Appl Energy 2016;167:366–76.
[44] Zeng B, An Y. Solving bilevel mixed integer program by reformulations and decomposition. Tech rep. University of South Florida; 2014.
[45] Aghaei J, Nezhad AE, Rabiee A, Rahimi E. Contribution of plug-in hybrid electric vehicles in power system uncertainty management. Renew Sustain Energy Rev 2016;59:450–8.
[46] GAMS/CPLEX solver manual. < http://www.gams.com > ; 2015.
[47] Li C, Xu Y, Yu X, Ryan C, Huang T. Risk-averse energy trading in multienergy microgrids: a two-stage stochastic game approach. IEEE Trans Ind Inform 2017;13(5):2620–30.
[48] Li C, Liu C, Deng K, Yu X, Huang T. Data-driven charging strategy of PEVs under transformer aging risk. IEEE Trans Contr Syst Technol 2017;PP(99):1–14.